Materials and Design 57 (2014) 330–335

Contents lists available at ScienceDirect

Materials and Design

journal homepage: www.elsevier.com/locate/matdes

Technical Report

Investigation of the low-speed impact behavior of dual particle size metal matrix composites

Afşın Alper Cerit *

Erciyes University, Engineering Faculty, Dept. of Industrial Design Engineering, 38039-Kayseri, Turkey

ARTICLE INFO

Article history:
Received 11 November 2013
Accepted 31 December 2013
Available online 10 January 2014

ABSTRACT

SiC-reinforced aluminum matrix composites were manufactured by powder metallurgy using either single or dual particle sized SiC powders and samples sintered under argon atmosphere. Quasi-static loading, low-speed impact tests and hardness tests were used to investigate mechanical behavior and found that dual particle size composites had improved hardness and impact performance compared to single particle size composites. Sample microstructure, particle distributions, plastic deformations and post-testing damages were examined by scanning electron microscopy and identified microstructure agglomerations in SPS composites. Impact traces were characterized by broken and missing SiC particles and plastically deformed composite areas.

© 2014 Elsevier Ltd. All rights reserved.

1. Introduction

Engineering materials must adequately fulfill their proposed function under working conditions, in which they will be exposed to various application-dependent impacts and loads. Visible damage can occur on metals and metal alloys as a result of impact, load induced stresses and plastic deformation [1,2]. Although metals are capable of absorbing large quantities of energy during impact, and therefore large unanticipated fragmentations generally do not occur, post-impact damage to composite materials is sometimes visible. In addition, non-obvious damage (e.g., delamination, fragmentation, detachment or loss of reinforced particles) can also occur. The extent of such damage is determined by the energy transferred during impact, making it important to establish material behaviors under impact [3–6]. Due to their low density, high elastic modulus, improve durability and favorable resistance to corrosion and wear, SiC-reinforced composites with aluminum matrix have been widely applied in automobile, space, plane and defense industries [7–15], however, the behavior of such composites under impact has yet to be fully characterized.

Impact velocity has been shown to result in increased contact force in aluminum- and SiC-reinforced functionally graded circular plates [16]. In aluminum composites using the LM13 alloy as matrix, dual reinforcement by ceramic particles (zircon sand, 3%; silicon carbide, 12%) exhibited the best wear resistance under all tested conditions [17]. In a study of the effects of various DPS composites upon wear and mechanical properties, improvements in wear resistance of DPS composites were attributed to the ability of larger SiC particles to carry a greater portion of the applied load, as well as an ability of the larger SiC particles to protect smaller SiC particles from being gouged out during the wear process [18]. In addition, grain reinforcement and dislocation strengthening mechanisms have been shown to have an important role in the improved yield strength of a DPS reinforced magnesium matrix composite, relative to SPS-reinforced composites [19]. Microscopic scale fracture has also been shown to contribute to cracking of individual and particle clusters within matrix and that particle cracking increased with reinforcement content in an aluminum alloy matrix [20]. Although static compression and impact tests in hybrid composite (graphite/epoxy glass) tubes found that the energy absorption and post crushing integrity of hybrid composite tubes were not superior to those of single material tubes [21], it has since been shown that total impact energy is an unfavorable parameter for direct material characterization in low-velocity impact testing of composite materials, and that impact force history is a much more relevant measure [22]. Static indentation tests represent the lower limit of impact velocity and for non-rate sensitive materials will give essentially the same results as a low-velocity impact test. For alumina and carbon fiber reinforced aluminum alloy matrix composites under low-velocity impact testing, it has been shown that as impact velocity increases, the impact energy absorbed by each of the materials increases, without significant change to dynamic fracture toughness [23].

Despite the numerous studies conducted in impact behavior of metal matrix composites, only limited data is available on the behavior of DPS composites. The present study focused on the impact behavior of powder metallurgy manufactured AA2124 matrix composites reinforced with various sized SiC particles. Composite samples were tested by static indentation and low-speed impact tests and sample hardness measured. SPS composites

* Corresponding author. Tel.: +90 (352) 2076666; fax: +90 (352) 4375784.
E-mail address: acerit@erciyes.edu.tr
URL: http://www.alpercerit.com

0261-3069/$ - see front matter © 2014 Elsevier Ltd. All rights reserved.
http://dx.doi.org/10.1016/j.matdes.2013.12.074

and unreinforced samples were manufactured and tested for comparison.

2. Materials and method

Aluminum 2124 series powders (24 μm diameter) were used as matrix material (Table 1) together with SiC particles as reinforcing material. To study the effects of SiC ceramic grain sizes and mixing proportions on the hardness and impact characteristics of composite materials, SiC reinforced (SPS and DPS) AA2124 matrix were manufactured. SPS composites were generated by addition of 10 vol.% of 2, 53 or 167 μm (SPS/2, SPS/53 and SPS/167) SiC ceramic particles to an AA2124 matrix, whereas DPS composites were manufactured by adding combinations of 2 and 53 μm (DPS/2-53), 2 and 167 μm (DPS/2-167), and 53 and 167 μm (DPS/53-167), SiC particles to AA2124 matrix at 10 vol.% (5% of each particle size). Unreinforced AA2124 samples were also manufactured for comparison. Sample codes and contents can be seen in Table 2.

A powder metallurgy process was used to manufacture metal matrix composite samples as follows and manufacturing parameters were determined in previous works [7,14,16,24,25]. Ceramic and metal powders were mixed for 1 h by an automatic mixer to achieve homogeneity. The mixed metal/ceramic powder was then placed into a circular die made of hot-work tool steel. The steel die containing the powder mixture was then placed into a furnace, which has a protective argon atmosphere (Fig. 1a). The composite samples sintered under a pressure of 300 MPa in a 3 lt/min argon flow at a temperature 615 °C for 30 min. Finally, composite samples were left to cool under a controlled pressure to avoid thermal deformation (Fig. 1b). The cylindrical specimens were produced with a 50 mm diameter and 12 mm thickness.

Impact tests were performed at the room temperature using a CEAST Fractovis testing machine. The impactor, with a hemispherical node, had a diameter of 20 mm and a strain-gauge force transducer of 40 kN. The specimens were clamped by an automatic clamping device from their edges (5 mm), therefore reducing the remaining free portions of the specimens to an inner diameter of 40 mm (Fig. 2). A total impact mass of 5.045 kg was used for the test unit.

The composite sample hardness was measured by the Brinell hardness test with a 10 mm ball and 3000 kg load. Hardness tests were performed by taking a minimum of 5 indentations per sample. Quasi-static tests were performed on the composite samples using a SHIMADZU AGX-50 universal testing machine. A quasi-static test plate consisting of a 20 mm steel ball was placed on the top jaw and samples placed on the bottom platen of the SHIMADZU universal testing machine. For all tests, the top indenter moved down to indent specimens at a velocity of 0.4 mm/s. The force and displacement of the indenter was automatically recorded by computer software connected to the testing machine. When all the tests had been completed, the samples were prepared for metallographic investigation using real-time metallographic techniques. The microstructures of the samples were observed by scanning electron microscopy (SEM).

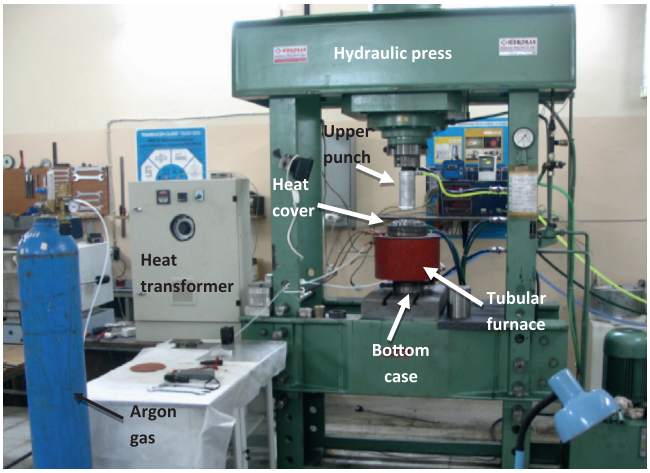
Table 1
Chemical composition of the aluminum alloy (wt%).

Material	Al	Cr	Cu	Fe	Mg	Mn	Si	Ti	Zn
AA2124	94.7	0.1	4.9	0.3	1.8	0.9	0.2	0.15	0.25

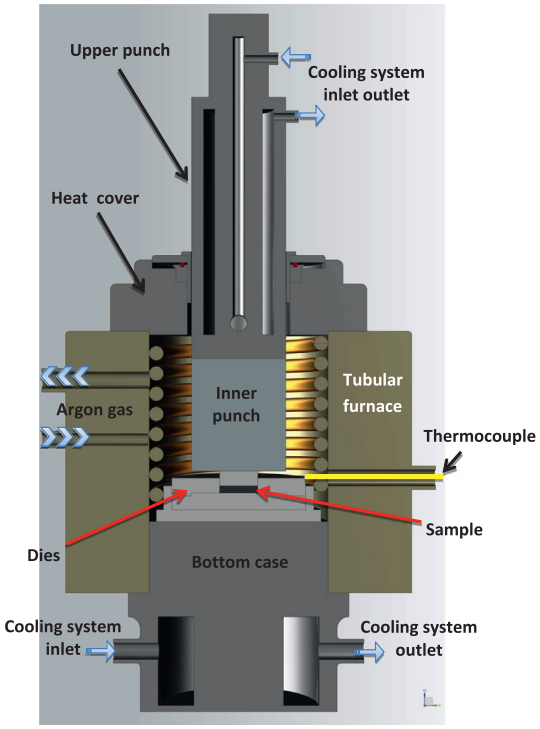
Table 2
Samples contents and ratios.

Symbol	SiC particle sizes (μm)	Volume fraction (%)
AA2124	–	Unreinforced
SPS/2[a]	2	10
SPS/53[a]	53	
SPS/167[a]	167	
DPS/2-53[a]	2 and 53	5 + 5
DPS/2-167[a]	2 and 167	
DPS/53-167[a]	53 and 167	

[a] Matrix material is AA2124 aluminum alloy powder.



(a)



(b)

Fig. 1. (a) Hot-press unit used for composite samples, (b) schematic view of die-tubular furnace.

3. Results and discussions

Samples microstructures were examined under a scanning electron microscopy and agglomerations could be observed in the microstructures of composite specimens containing 2 μm sized

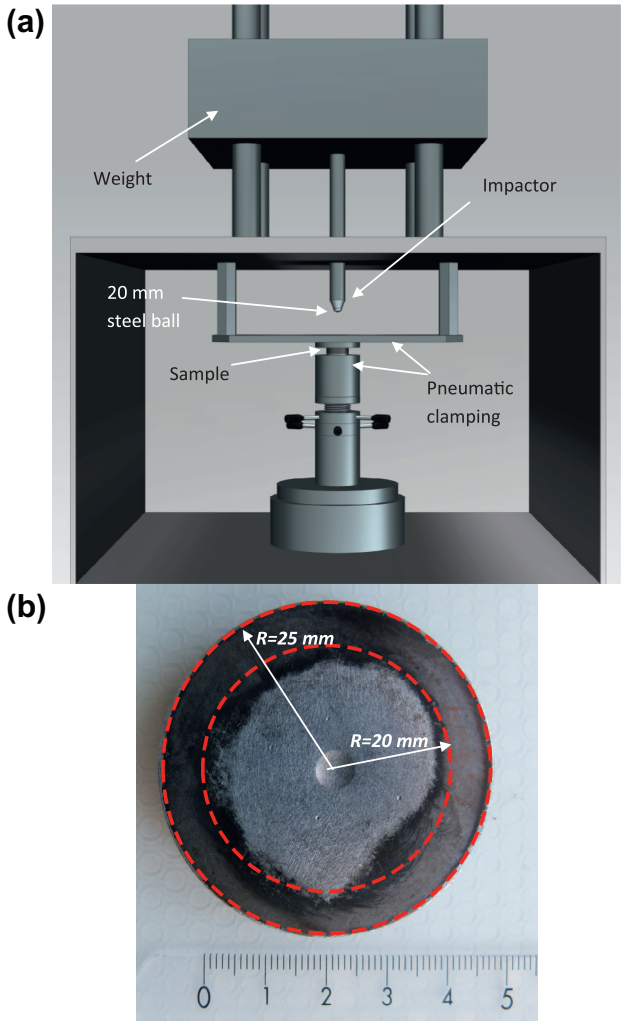


Fig. 2. (a) Impact test fixture, (b) clamped and free parts of composite samples.

SiC reinforcement (SPS/2 and DPS/2-53) (Figs. 3 and 4). The resulting microstructure irregularities caused by agglomerations had an adverse impact on material strength. In addition to their direct effects on the mechanical features, an increase in reinforcement particle grain size produced a more homogenous distribution in the microstructure, which is thought to be achieved by preventing agglomeration of the smaller grain particles. In the DPS/2-53 specimens, we could observe a homogenous distribution of the larger particles, while the smaller particles form sporadic clusters (Fig. 4). A homogenous distribution was observed in the microstructure of DPS/53-167 and DPS/2-167 composite specimens, in which larger (167 μm) particles had been used (Fig. 5). This suggests that the larger 167 μm particles are able to prevent agglomeration of the smaller particles (Fig. 6).

Impact testing was performed using impactor hitting the surface of the sample, which transfers 10.85 J of energy onto the surface of the material during impact. The Brinell hardness scores (HB10/3000) of the SiC-reinforced SPS specimens were recorded as 122 (2 μm), 142 (53 μm) and 109 (167 μm) HB, while the hardness of un-reinforcement AA2124 was 105 HB (Fig. 7a). Whereas DPS samples had hardness values of 111 (DPS/2-53 μm), 142 (DPS/2-167 μm) and 121 (DPS/53-167 μm) HB (Fig. 7b). Although it has been determined that large particle sizes reduce hardness in single sized reinforced composites [26], we observed the opposite trend in DPS composites, possibly due to difficulties associated

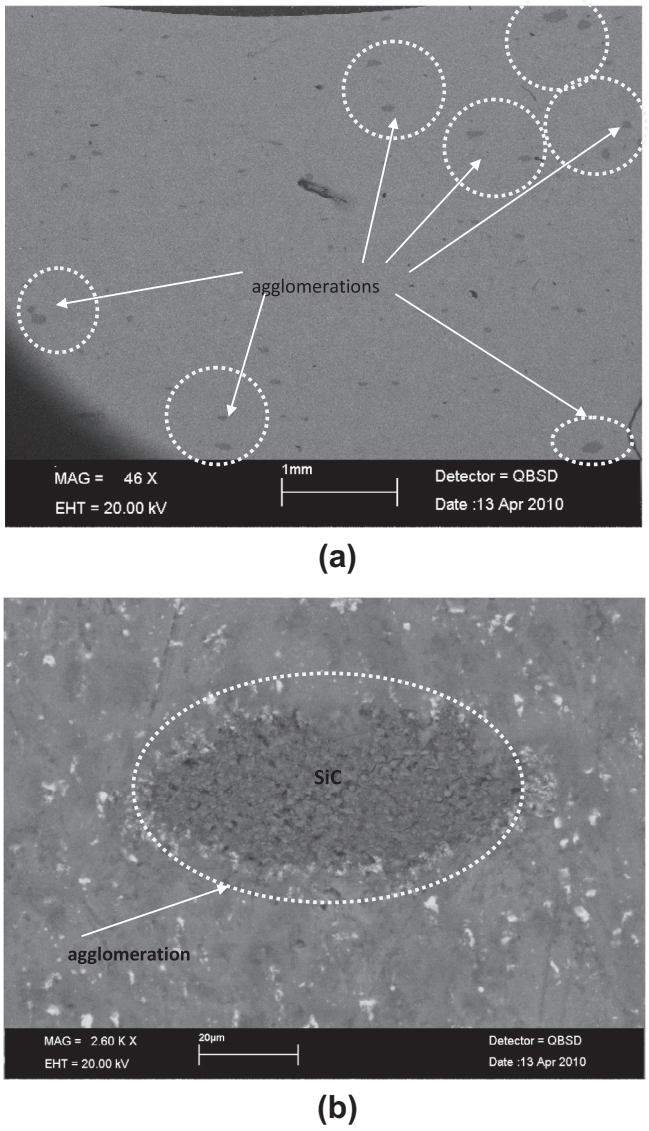


Fig. 3. (a) Microstructure of SPS/2 composite sample, (b) detail view of the SiC agglomeration.

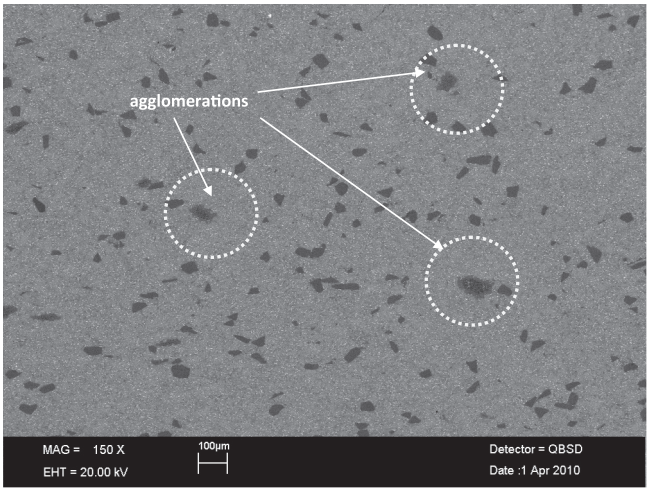


Fig. 4. Agglomerations and microstructure of DPS/2-53 composite sample.

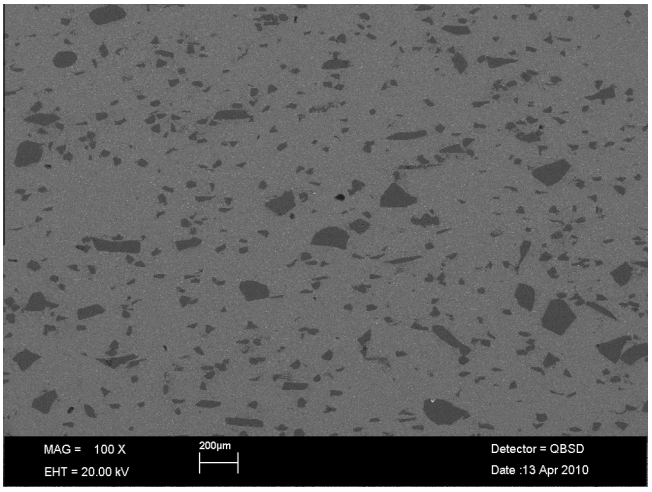


Fig. 5. Particle distribution in the DPS/53-167 composite sample.

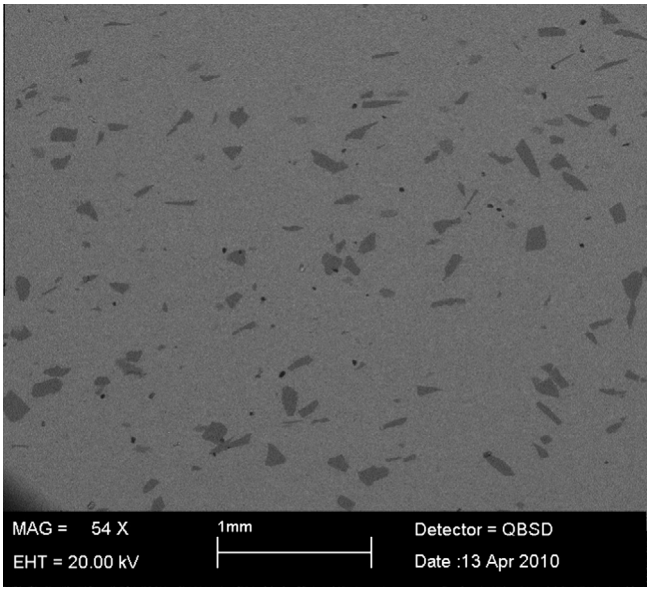


Fig. 6. Microstructure of the DPS/2-167 composite sample.

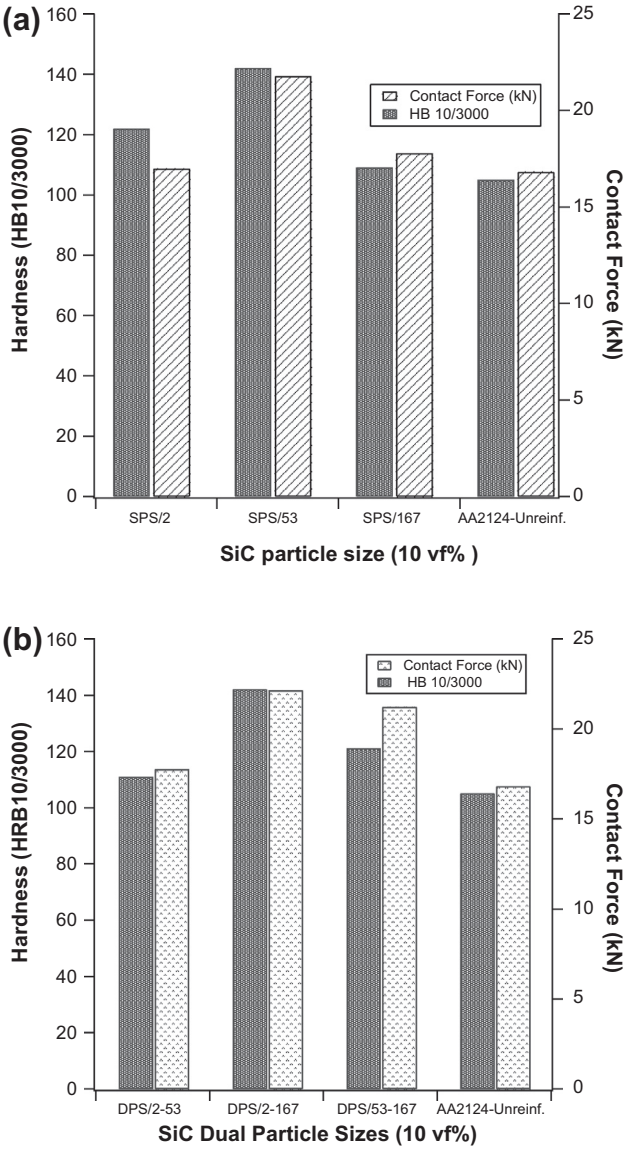


Fig. 7. Hardness-contact force graphs of (a) single particle size composites, (b) dual particle size composites.

with manufacturing and agglomeration. The hardness values of the DPS samples containing 167 µm particles (DPS/2-167 and DPS/53-167) are greater than that of the DPS/2-53 sample, because larger particles help to carry a greater portion of the applied load [18], also due to the presence of agglomerations in the microstructure of DPS/2-53. The contact forces of SiC-reinforced SPS composite samples measured 16.99 (2 µm), 21.77 (53 µm) and 17.78 kN (167 µm), while that of the unreinforced sample was 16.8 kN (Fig. 7a). For the DPS samples, contact forces of 17.75 (DPS/2-53), 22.14 (DPS/2-167) and 21.22 kN (DPS/53-167) were recorded (Fig. 7b). The contact force of all specimen types was correlated with the hardness values; the contact forces of harder samples were higher than in softer samples, as expected.

Post-impact test contact force-time graphics reveal that the 53 µm containing sample had the highest contact force amongst SPS and unreinforced samples. In fact, the contact force of SPS/53 was able to reach levels as high as 2.25 ms and retain the ability to return to zero level (Fig. 8a). As samples with low contact force and hardness possess greater ductility, their contact times are longer (2.6–2.75 ms). The maximum contact force values of the DPS samples were less variable and, for samples DPS/2-167 and DPS/53-167, were correlated to sample hardness [27]. While the contact times of the DPS/2-53 sample was the same as unreinforced AA2124 (2.75 ms), contact times of 2.3 ms were recorded for the DPS/2-167 and DPS/53-167 samples (Fig. 8b).

As the speed of the impactor during the impact testing is fixed, its kinetic energy at the time of impact can be calculated as 10.85 J. At the moment of impact, some of the impactors kinetic energy is absorbed by the material for elastic and plastic deformation [27]. As seen in the kinetic energy time graphics, of the 10.85 J input energy, 4.5–4.7 J are converted into output energy (Fig. 9). This disparity between input and output energies represents a 50–60% energy absorption by the samples. As such, all samples can be said to possess similar energy characteristics, differing by only ~10% across all samples tested (Fig. 9).

Examination of impact traces and their surrounding areas by SEM reveals deep dents resulting from plastic deformation of the matrix (Figs. 10 and 11). It was also seen that the reinforcing SiC ceramics on the surface and in the superficial areas had been shattered (Figs. 10 and 11).

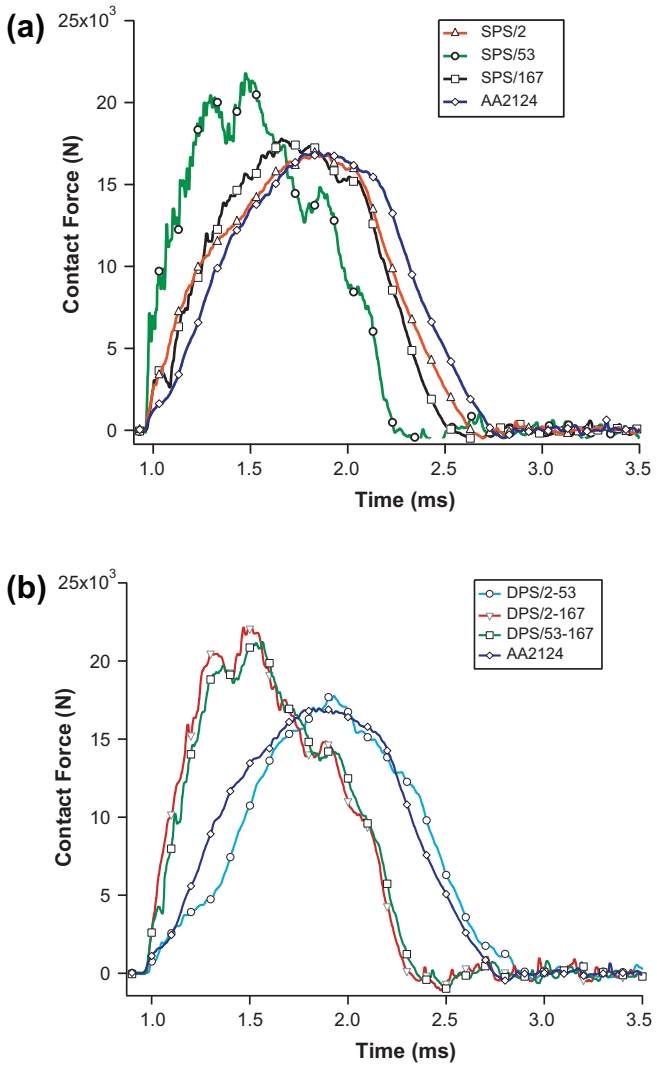


Fig. 8. Contact force-time graphs of (a) single particle size composites, (b) dual particle size composites.

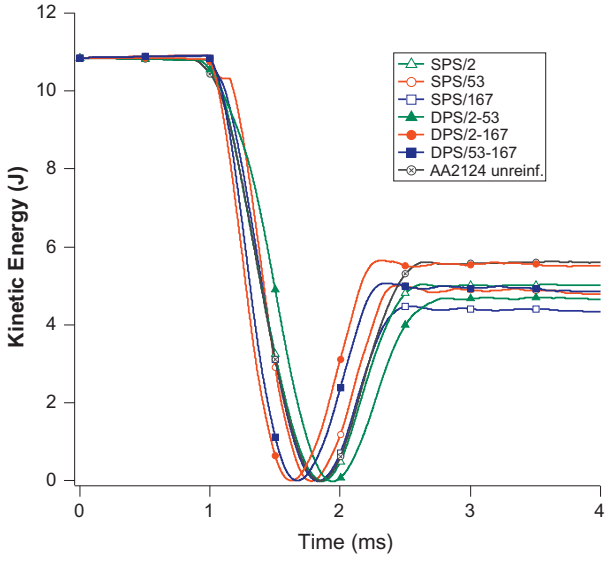


Fig. 9. Kinetic energy histories of impactor.

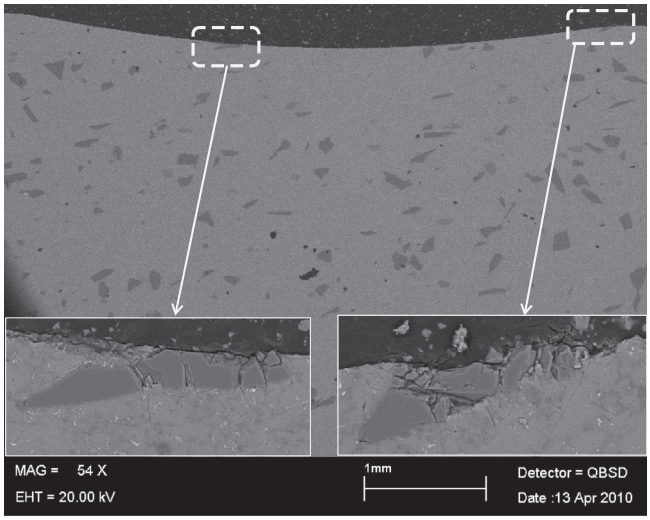


Fig. 10. Plastic deformation and SiC damages on the DPS/2-167 sample surface.

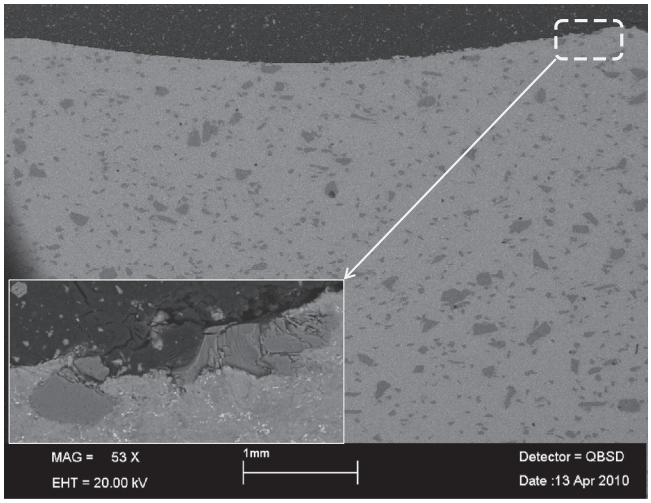


Fig. 11. Plastic deformation and SiC damages on the DPS/53-167 sample surface.

In addition static loading test were performed by indenting a 20 mm steel ball into the material to a depth of 2 mm. When the force/displacement graphics are studied, it can be seen that in SPS composites the greatest resistance to the applied force was measured for the 53 μm containing sample (Fig. 12a). In DPS -reinforced composites, the DPS/2-167 sample (which is the hardest and possesses the greatest contact force) displays the greatest resistance, followed by DPS/53-167 and DPS/2-53. Unreinforced AA2124 displayed the least resistance of all samples.

4. Conclusions

In this study the effects of SiC ceramic grain sizes and mixing proportions on the hardness and impact characteristics of composite materials were studied. The following conclusions can be drawn from the results of the present study performed on dual and single particle sized reinforced composites.

Agglomerations have occurred in the microstructure of the small particle sized reinforced composites, which have negatively affected the hardness and impact behavior. We found that as the size of the reinforcement increases the microstructure heterogeneity increases. It has been observed that, in dual particle reinforced

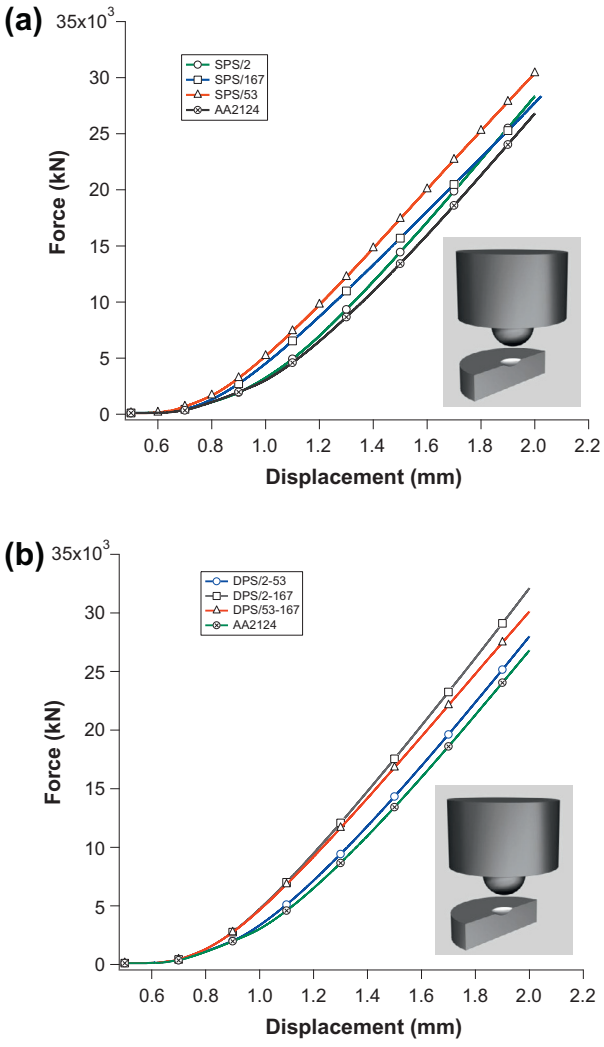


Fig. 12. Force–displacement graphs of (a) single particle size composites, (b) dual particle size composites.

composites, large particles prove useful in preventing agglomerations.

The hardness level, as well as static and impact behaviors, of 53 μm SiC-reinforced aluminum matrix is most favorable; although force decreases in proportion to contact force, contact time is increased. The 167/2 μm DPS SiC-reinforced composites were identified as the next most favorable materials. As expected, unreinforced AA2124 displayed the lowest hardness, contact force and longest contact duration, which can be accounted for by its ductility.

The increased hardness of the 2 and 167 μm containing DPS composite was accompanied by the highest force in static and dynamic loadings. The 2/167 and 53/167 μm containing DPS samples behaved similarly. All DPS-reinforced composites possess similar curves of resistance to static force loading, and of these samples, DPS/2-167 had the greatest resistance of static load.

The impact behaviors of the DPS composites were more favorable than those of SPS-reinforced composites. It is thought that the DPS-reinforced composites reacted to the applied force with similar curvilinear changes as SPS samples, but with favorable interactions between particle classes, thus increasing strength.

Kinetic energy–time graphics demonstrate that 50–60% of input energy was absorbed by the samples and that this parameter was similar across all tested samples.

SEM analyses of the impact traces and microstructure reveal that surface (or close to surface) SiC particles have been shattered and detached under impact.

References

[1] Richardson MOW, Wisheart MJ. Review of low-velocity impact properties of composite materials. Compos A Appl Sci Manuf 1996;27:1123–31.
[2] Hosseinzadeh R, Shokrieh MM, Lessard L. Damage behavior of fiber reinforced composite plates subjected to drop weight impacts. Compos Sci Technol 2006;66:61–8.
[3] Park H, Changduk K. A study on low-velocity impact damage evaluation and repair technique of small aircraft composite structure. Composites A 2011;42:1179–88.
[4] Dale M, Acha AB, Carlsson LA. Low-velocity impact and compression after impact characterization of woven carbon/vinyl ester at dry and water saturated conditions. Compos Struct 2012;94:1582–9.
[5] Shi Y, Swait T, Soutis C. Modelling damage evolution in composite laminates subjected to low-velocity impact. Compos Struct 2012;94:2902–13.
[6] Sevkat E, Liaw B, Delale F. Drop-weight impact response of hybrid composites impacted by impactor of various geometries. Mater Des 2013;52:67–77.
[7] Karamış MB, Cerit AA, Selçuk B, Nair F. The effects of different ceramics size and volume fraction on wear behavior of Al matrix composites (for automobile cam material). Wear 2012;163:51–9.
[8] Guobin L, Jibing S, Quanmei G, Hemin D, Jianwei L, Zhenyan Z. Wear of Al–Mg–Cu composite reinforced by in situ formation of ceramics. J Mater Process Technol 2005;170:416–20.
[9] Zawrah MF, Aly MH. In situ formation of Al_2O_3–SiC–mullite from Al-matrix composites. Ceram Int 2006;32:21–8.
[10] Ahn JJ. The effect of wear environment temperature on the wear behavior and friction coefficient of SiCw/Al composite. J Compos Mater 2003;37:1083–19093.
[11] Omar MF, Akil HM, Ahmad ZA. Particle size-dependent on the static and dynamic compression properties of polypropylene/silica composites. Mater Des 2003;45:539–47.
[12] Yan YW, Gerng L, Li AB. Experimental and numerical studies of the effect of particle size on the deformation behavior of the metal matrix composites. Mater Sci Eng, A 2007;448:315–25.
[13] Yang LJ. A methodology for the prediction of standard steady-state wear coefficient in an aluminum-based matrix composite reinforced with alumina particles. J Mater Process Technol 2005;162–163:139–48.
[14] Karamış MB, Cerit AA, Nair F. Surface characteristics of projectiles after frictional interaction with metal matrix composites under ballistic condition. Wear 2006;261:738–45.
[15] Ozden S, Ekici R, Nair F. Investigation of impact behaviour of aluminium based SiC particle reinforced metal matrix composites. Compos A Appl Sci Manuf 2007;38:484–94.
[16] Güneş R, Aydın M, Apalak MK, Reddy JN. The elasto-plastic impact analysis of functionally graded circular plates under low-velocities. Compos Struct 2011;93:860–9.
[17] Kumar S, Panwar SR, Pandey OP. Effect of dual reinforced ceramic particles on high temperature tribological properties of aluminum composites. Ceram Int 2013;39:6333–42.
[18] Bindumadhavan PN, Wah HK, Probhakar WO. Dual particle size (DPS) composites: effect on wear and mechanical properties of particulate metal matrix composites. Wear 2001;248:112–20.
[19] Deng K, Shi J, Wang C, Wang X, Wu Y, Nie K, et al. Microstructure and strengthening mechanism of bimodal size particle reinforced magnesium matrix composite. Composites A 2012;43:1280–4.
[20] Srivatsan TS, Prakash A. The quasi-static fracture behavior of an aluminum alloy metal matrix composite. Compos Sci Technol 1995;53:307–15.
[21] Farley GL. Energy absorption of composite materials. J Compos Mater 1983;17:267–79.
[22] Sjöblom OP, Hartness JT. On low-velocity impact testing of composite materials. J Compos Mater 1988;22:30–52.
[23] Nam HW, Aggag AG, Takahashi K, Han KS. The dynamic behavior of metal matrix composites under low-velocity impact. Compos Sci Technol 2000;60:817–23.
[24] Cerit AA, Karamış MB, Nair F, Yıldızlı K. Effect of reinforcement particle size and volume fraction on wear behavior of metal matrix composites. J Balkan Tribol Assoc 2008;12–4:482–9.
[25] Karamış MB, Sarı FN, Erturun V. Friction and wear behaviors of reciprocatingly extruded Al–SiC composite. J Mater Process Technol 2012;212:2578–85.
[26] Stone IC, Tsakiropoulos P. The effect of the spatial distribution of reinforcement on the fabrication and heat treatment of (Al–4 wt% Cu)SiC particle metal matrix composites. Mater Sci Eng, A 1994;189:285–90.
[27] Apalak MK, Güneş R, Aydın M, Reddy JN. Impact performance of Al/SiC functionally graded circular plates. Int. J. Mater Prod Technol 2011;42:56–65.